Journal of Hydrology: Regional Studies 6 (2016) 66–81

Contents lists available at ScienceDirect

Journal of Hydrology: Regional Studies

journal homepage: www.elsevier.com/locate/ejrh

Impacts of recent climate change on the hydrology in the source region of the Yellow River basin

Fanchong Meng[a,b], Fengge Su[a,c,*], Daqing Yang[d], Kai Tong[a], Zhenchun Hao[e]

[a] Key Laboratory of Tibetan Environment Changes and Land Surface Processes, Institute of Tibetan Plateau Research, Chinese Academy of Sciences, Beijing, China
[b] University of Chinese Academy of Sciences, Beijing, China
[c] CAS Center for Excellence in Tibetan Plateau Earth Sciences, Beijing, China
[d] National Hydrology Research Center, Environment Canada, Saskatoon, Saskatchewan, Canada
[e] State Key Laboratory of Hydrology—Water Resources and Hydraulic Engineering, Hohai University, Nanjing, China

ARTICLE INFO

Article history:
Received 5 July 2015
Received in revised form 25 March 2016
Accepted 28 March 2016
Available online 11 April 2016

Keywords:
Climate change
Hydrology
Snow
Source region of the Yellow River

ABSTRACT

Study region: The source region of the Yellow River (SRYE) in the northeastern Tibetan Plateau.
Study focus: The spatial-temporal changes of hydrological and meteorological variables and their linkages over the SRYE were investigated for 1961–2013. Meanwhile, we quantified the impacts of precipitation and evapotranspiration on hydrological changes through climate elasticity by applying a land surface hydrological model. Furthermore, the impacts of warming climate on the seasonal snow cover and spring flow over the SRYE were examined.
New hydrological insights for the region: Decreased precipitation and lightly increased evapotranspiration both contributed to reduced runoff in the 1990s, with the decreased precipitation playing a more important role (70%) than the increased evapotranspiration (30%). In the 2000s, precipitation contributed 3% to the runoff reduction, while the increased evapotranspiration accounted for 97%. Along with rapid warming, evapotranspiration is playing an increasingly important role in affecting runoff changes in the SRYE. During 2001–2012, snow cover in May decreased over the region. Spring peak flow mainly caused by snowmelt occurred earlier for about 15 days at the Jimai hydrological station due to an earlier snow melt associated with the climate warming in the past 3 decades.

1. Introduction

The Yellow River originates from the Tibetan Plateau (TP), and flows across eight provinces from west to east across China (Fig. 1). It is 5464 km long with a basin area of 752,443 km^2, the sixth longest river in the world and the second in China (Fu et al., 2004). The Yellow River plays an important role not only in the water supply for 107 million people (Wang et al., 2006) but also in the agricultural production in China because 13% of the countries' total cultivated area depends on the water resources from this basin (Cai and Rosegrant, 2004). The drainage area upstream of the Tangnaihai (TNH) hydrological station (Fig. 1), located in the northeast of the TP, is generally considered as the source region of the Yellow River (SRYE) basin. The SRYE is the "water tower" of the Yellow River basin since it contributes about 35% of total annual runoff from

* Corresponding author at: Key Laboratory of Tibetan Environment Changes and Land Surface Processes, Institute of Tibetan Plateau Research, Chinese Academy of Sciences, Beijing, China.
E-mail address: fgsu@itpcas.ac.cn (F. Su).

http://dx.doi.org/10.1016/j.ejrh.2016.03.003

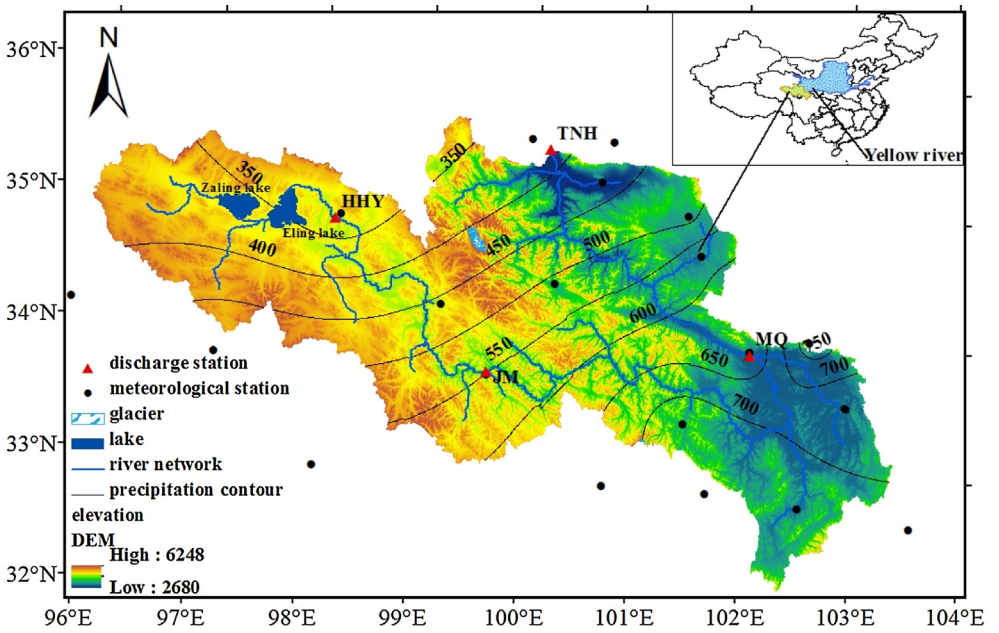

Fig. 1. Location and topography of the source region of the Yellow river (SRYE). Red triangles denote discharge stations. From up to downstream, these are Huangheyan (HHY), Jimai (JM), Maqu (MQ) and Tangnaihai (TNH) stations, respectively. Black points represent meteorological stations. Mean annual precipitation contours (mm) are also indicated. (For interpretation of the references to color in this figure legend, the reader is referred to the web version of this article.)

about 16% of the basin area (Lan et al., 2010b). Therefore, it is of vital importance in meeting downstream water resources requirements (Zheng et al., 2007).

Similar to other regions, climate change is taking place in the Yellow River basin (Wang et al., 2014; Yang et al., 2004; Zhao et al., 2007). Studies of long term climatic records suggested a noticeable warming trend of 0.31–0.35 °C/10yr over the SRYE in the past 5 decades (Cuo et al., 2013; Hu et al., 2011; Lan et al., 2010b). No significant long-term trends have been observed in the basin-wide precipitation (Hu et al., 2012), although large decadal and spatial variations in precipitation exist in this region (Lan et al., 2010b; Zhou and Huang, 2012). Along with the changing climate, mean annual flow at the TNH has decreased in the past 50 years (Cuo et al., 2013; Hu et al., 2011; Lan et al., 2010b; Li et al., 2012). It has been noted that the flow in the 1990s suffered a serious decrease in this region (Chen et al., 2007), accompanied with an increase in the number of zero-flow days at the most upstream gauging site—the Huangheyan (HHY, Fig. 1) station (Zhang et al., 2004a). Attempts have been made to understand the causes of the changes in streamflow over the SRYE (Cuo et al., 2013; Hu et al., 2011; Lan et al., 2010a; Zhao et al., 2009; Zhou and Huang, 2012). It is generally recognized that the hydrological changes are mostly attributed to climate change and climate variability. Studies show that changes in seasonal and spatial distribution of precipitation played an important role in regional hydrology (Hu et al., 2011; Lan et al., 2010a; Zhou and Huang, 2012). However, it is still not clear to what extent precipitation and the climate warming affected the streamflow regimes over the region.

Through statistical analysis, Hu et al. (2011) suggested that decreased precipitation in the wet season and rising temperature over the period 1959–2008 may be responsible for the general flow reduction over the SRYE. Sato et al. (2008) developed a new hydrological model to investigate the water balance of the SRYE basin during 1960–2000. Although an increase in evapotranspiration was detected, they concluded that the decrease in precipitation was the main factor for the decrease in river discharge. Zhou and Huang (2012), using a point scale land surface model and surface meteorological observations for 1960–2006, investigated the influences of climatic changes on the water budget over the SRYE. Their results suggested that the changes in spatial precipitation pattern was an important factor for streamflow changes. In addition, increase in evapotranspiration due to rising temperature was another cause for runoff decrease.

Although hydrologic response to climate changes over the SRYE has been intensely discussed, most of the investigations focused on statistical analyses of the long-term trends in precipitation, temperature and runoff (Hu et al., 2012, 2011; Zhao et al., 2007; Zheng et al., 2007). Few studies quantitatively examined physical mechanisms and processes of hydrological changes and variations (Cuo et al., 2013; Zheng et al., 2009). Furthermore, most studies focused on change detections at individual stations in a basin or region (Hu et al., 2012; Wang et al., 2014; Zhou and Huang, 2012), rather than spatial analyses over the basins. The causes for discharge changes over the SRYE seem controversial. Thus, a comprehensive study to quantify temperature and precipitation changes and their impacts on streamflow changes over time and space is necessary.

Rising temperatures may lead to earlier snow melt and runoff over the cold regions (Barnett et al., 2005; Stewart, 2009). Snow melt contributes 40% of spring runoff (Lan et al., 1999) and 5–13% of annual runoff (Cuo et al., 2013) in the SRYE. It

is therefore important to understand how snowcover and snow melt runoff responded to climate warming in this region. Studies on snow cover in the TP exist (Qin et al., 2006; Zhang et al., 2004b), but only few focused on the source region of the Yellow River (Lu et al., 2009; Yang et al., 2007).

In this work, we provided an update on the impacts of climate change to the hydrology of the SRYE during 1961–2013. We applied a large scale land surface hydrology model to quantify evapotranspiration changes. The specific objectives are: 1) to investigate the spatial-temporal changes of runoff, precipitation and temperature, as well as the linkage between runoff and climate variables; 2) to quantify the impacts of precipitation and temperature variations on the hydrological changes through climate elasticity by applying the land surface hydrological model; and 3) to examine the impacts of climate warming on the seasonal snow cover and spring flow over the SRYE.

2. Study area

The SRYE, located in the region between 95°50′E–103°30′E and 32°N–35°40′N (Fig. 1), has an area of 121,972 km^2, and annual runoff of 2.04×10^{10} m^3, accounting for 34.5% of total annual runoff of the Yellow River basin. It originates from the Bayan Har mountains, with the altitude ranging between 2680 m and 6248 m above sea level and decreasing towards the east. The land surface in this region is characterized by glaciers, snow, lakes and frozen soils. The vegetation type is mostly grassland, covering 80% of this region (Zheng et al., 2009). The highest elevation is found at the Anyemaqen Mountains, with permanent snow cover and 58 glaciers, accounting for 95.8% of total glacier areas (134 km^2) over the SRYE. Since glacier occupies only about 0.11% of the basin (Zhang et al., 2013), it is not considered in this work. There are four hydrological stations in the mainstream of the SRYE: Huangheyan (HHY), Jimai (JM), Maqu (MQ), Tangnaihai (TNH) (Fig. 1). The HHY, with mean annual runoff of 4.41×10^8 m^3 (Zhang et al., 2012), contributes less than 5% of the total flow at TNH. Due to small flow contribution and the missing streamflow data during 1969–1975, data from HHY were not used in the analysis. We divided the SRYE into three regions, the region upstream of Jimai (JM) hydrological station, between JM and MQ (JM-MQ), and between MQ and TNH (MQ-TNH). The region JM-MQ (Fig. 1) is the major runoff generation area, with a runoff ratio of 0.38 and a contribution of 51% to the total flow at the TNH. The regions upstream of JM and MQ-TNH are relatively dry with runoff ratios of 0.21–0.34 and contributing 21% and 28% to the total flow, respectively. There are about 5300 lakes with a total area of 2000 km^2 over the SRYE (Hu et al., 2011), of which more than 4000 lakes are located above the HHY (Li et al., 2013). The Zaling and Eling lakes are the two largest ones, with areas of 550 km^2 and 610 km^2, respectively (Fig. 1) (Hu et al., 2011). Because there are no large dams in the region and the population density is low, human activities and their impacts to basin hydrology were not considered in this work.

The average annual precipitation over the SRYE is about 522 mm, ranging from 350 mm in the northwest to 750 mm in the southeast (Fig. 1). About 75–90% of precipitation falls in the wet season (June–September) due to the southeast monsoon from the Bay of Bengal (Zheng et al., 2009). The mean annual temperature varies between −4 °C and −2 °C from the northwest to the southeast (Hu et al., 2011). January is the coldest month, and the temperature stays below 0 °C from October to April; the warmest month is July, with a mean temperature of 8.0 °C.

3. Datasets and methodology

3.1. Data

The daily streamflow data collected at the three hydrological stations (JM, MQ and TNH; Fig. 1) were obtained from the Yellow River Conservancy Commission (YRCC). The flow data are available during 1961–2009 for the JM and MQ, and during 1961–2013 for the TNH. The daily meteorological data (1961–2013) including the maximum temperature (Tmax), the minimum (Tmin), temperature, precipitation and wind speed from 20 climate stations over the SRYE and the surrounding areas (Fig. 1) were obtained from the China Meteorological Administration (CMA). The daily Tmax, Tmin, precipitation and wind speed for these stations were interpolated to obtain $1/12^\circ \times 1/12^\circ$ grids data through the inverse distance weighting method. The temperature was adjusted for elevation by applying a common temperature lapse rate (0.6 °C/100 m) for interpolation from points to grids.

The global 8-day and 0.05° Moderate Resolution Imaging Spectroradiometer (MODIS) snow products (MOD10C2) (http://nsidc.org/data/modis/index.html) during 2001–2012 were used for snow cover analysis.

The terrestrial water storage (TWS) was estimated from the Gravity Recovery and Climate Experiment (GRACE) satellite launched in March 2002 (Tapley et al., 2004). GRACE products have shown a remarkable prospect in water mass change (Wahr et al., 2004). There are three institutes which officially provide GRACE products: the Center for Space Research (CSR) at the University of Texas at Austin, GeoForschungsZentrum (GFZ) and Jet Propulsion Laboratory (JPL). The GRACE data can be accessed from http://www.csr.utexas.edu/grace/. In this study, the GRACE RL5.0 monthly solutions from CSR for 2004–2013 were used to derive the evapotranspiration over the SRYE. The CSR products provide monthly anomalies of total TWS at $1^\circ \times 1^\circ$grids. The GRACE data have been widely used in estimating the terrestrial water storage change (TWSC) (Swenson et al., 2006; Syed et al., 2008) and in deriving other hydrological variables (Morrow et al., 2011; Ramillien et al., 2006; Rodell

et al., 2004). With the P, R and GRACE data, it is possible to calculate the evapotranspiration (ET) through the water balance equation:

$$ET = P - R - \Delta W; \quad (1)$$

where P is precipitation (mm), R is runoff (mm), and ΔW (mm) is the Terrestrial water storage change (TWSC), which is the difference of two sequential GRACE solutions.

3.2. Hydrological model

A large-scale land surface hydrological model named as the Variable Infiltration Capacity (VIC) (Liang et al., 1994, 1996; Lohmann et al., 1998) has been used in this work. The VIC model, a grid-based land surface model, parameterizes the dominant hydrometeorological processes taking place at the land surface-atmosphere interface. The model solves both water and energy balance for individual grid cells. A mosaic representation of land cover and the variable infiltration capacity curve accounting for subgrid heterogeneity in saturated extent are used in the VIC model. Through a channel network, surface runoff and base flow for each grid cell are routed to the basin outlet (Lohmann et al., 1998). The VIC model has the capacity to simulate cold region hydrology because it adopts a two layer energy balance snow model (Cherkauer and Lettenmaier, 1999; Storck and Lettenmaier, 1999) which represents snow accumulation and ablation and a frozen soil/permafrost algorithm (Cherkauer and Lettenmaier, 1999, 2003) that solves for soil ice contents. For the VIC model, a routing scheme is used to obtain the daily simulated hydrograph at the outlets. Topography data were obtained from SRTM (resolution: 90 m × 90 m) (http://srtm.csi.cgiar.org/SELECTION/inputCoord.asp). The DEM (digital elevation model) data were used to create the flow direction file which is needed in the routing scheme at the 1/12° × 1/12° grids.

The evapotranspiration (ET) in the VIC model consists of three components: canopy evaporation, transpiration and evaporation from bare soils (Liang et al., 1994). The ET was calculated as follows:

$$ET = \sum_{n=1}^{N} C_v[n] \times (E_c[n] + E_t[n]) + C_v[N+1] \times E_1 \quad (2)$$

where N is the land cover classes; Cv[n] is the fraction of the n_{th} vegetation type within a grid cell, and $C_v[N+1]$ is the fraction of bare soil with $\sum_{n=1}^{N} C_v[n] = 1$. $E_c[n]$ and $E_t[n]$ are the canopy evaporation and transpiration for the n_{th} land cover type, respectively. E_1 is the evaporation from bare soils. E_c, E_t and E_1 are estimated as a function of potential evaporation (E_P) based on the Penman-Monteith equation and other parameters related to vegetation type and soil moisture. In this work, evapotranspiration from the water balance Eq. (1) was used to compare with the evapotranspiration from the VIC model.

Zhang et al. (2013) set up a modeling framework at a 1/12° × 1/12° spatial resolution over the entire Tibet plateau. In this study, the VIC model setup for the SRYE was adopted from Zhang et al. (2013) including soil and vegetation parameters. Vegetation types were obtained from the University of Maryland's (UMD) 1 km Global Land Cover product (Hansen et al., 2000). The land cover type was considered to be fixed during the model simulation period 1961–2013. Therefore, the annual variation of simulated ET is mostly controlled by meteorological variables.

3.3. Statistical analysis

The discharge data were used to evaluate the VIC model simulations, the calibration has two criteria: relative error (Er) and Nash-Sutcliffe efficiency (E_{NS}) (Nash and Sutcliffe, 1970), which describes the prediction skill of the simulated streamflow relative to the observations. The E_{NS} and Er was computed from the following equations:

$$E_{NS} = 1 - \frac{\sum_{m=1}^{M} \left(Q_m^{obs} - Q_m^{sim}\right)^2}{\sum_{m=1}^{M} \left(Q_m^{obs} - \bar{Q}\right)^2} \quad (3)$$

$$E_r = \frac{\sum_{m=1}^{M} \left(Q_m^{sim} - Q_m^{obs}\right)}{\sum_{m=1}^{M} Q_m^{obs}} \times 100\% \quad (4)$$

Table 1
Recommended statistics for simulation performance ratings (Moriasi et al., 2007).

Rating	E_{NS}	Er(%)
Excellent	$0.75 < E_{NS} \leq 1.00$	$\mid Er \mid < 10$
Good	$0.65 < E_{NS} \leq 0.75$	$10 \leq \mid Er \mid < 15$
Satisfactory	$0.50 < E_{NS} \leq 0.65$	$15 \leq \mid Er \mid < 25$
Unsatisfactory	$E_{NS} \leq 0.50$	$\mid Er \mid \geq 25$

where the Q_m^{obs} means the observed monthly streamflow, and the Q_m^{sim} is the simulated discharge; $\bar{Q}$ is the observed mean monthly streamflow; M is the number of months. An E_{NS} value closer to 1 and Er closer to 0 imply better simulation results; see Table 1 for the simulation performance ratings applied in this study (Moriasi et al., 2007).

The precipitation, temperature and runoff values were normalized by subtracting their time series mean values and dividing by their standard deviations. Linear trend analysis through simple regression allowed us to investigate long-term changes of the historical data. In this method, the sum of squared residuals as the difference between the observed values and the fitted values is minimized. The statistical significance of the trends in this study was set at the 10% level.

Correlation analysis was used to examine the strength and direction of the relationship between the hydrological and meteorological variables. The correlation coefficient (r) is calculated using the Pearson method. The statistical significance of the correlations was again set at the 10% level.

Climate elasticity, proposed by Schaake (1990), was applied to evaluate the sensitivity of streamflow to climate change (Fu et al., 2007; Sankarasubramanian et al., 2001; Yang and Yang, 2011). More specifically, the relative contribution of precipitation and evapotranspiration changes to runoff changes was quantified where evapotranspiration instead of temperature was considered since evapotranspiration better represents the effects of climate change on basin water balance (Zheng et al., 2009). On the long term, the basin water storage changes can be neglected, thus the basin water balance can be represented as:

$$R = P - ET; \tag{5}$$

Without considering the impacts of human activity, the changes of runoff between two periods (ΔR) can be estimated as:

$$\Delta R = \Delta R_P + \Delta R_{ET}; \tag{6}$$

where ΔR_P and ΔR_{ET} are changes in runoff due to precipitation and evapotranspiration changes, respectively. ΔR can be estimated as follows (Dooge et al., 1999; Liu et al., 2012):

$$\Delta R = \Delta R_P + \Delta R_{ET} = (\varepsilon_p \Delta P/P + \varepsilon_{ET} \Delta ET/ET)R; \tag{7}$$

where ΔP and ΔET are the changes of P and ET between two periods. ε_P and ε_{ET} are the climate elasticity of P and ET to runoff, which implies that 1% change in P or ET induces ε% change in R (Tang et al., 2013). In this study, two periods 1990s and 2000s relative to 1960–1990 were considered. Since streamflow data at the JM and MQ were only available to 2009, we define the period 2001–2009 as the 2000s. Eq. (7) was set up for each period and the values for ε_P and ε_{ET} computed from the two equation, to obtain the impact of P and ET changes on runoff.

4. Precipitation, temperature, and runoff changes

4.1. Long-term changes

Fig. 2 displays annual time series of normalized runoff, regional mean precipitation and temperature for the basins upstream of the JM, MQ and TNH stations during 1961–2013. Precipitation shows positive trends for all the basins (Fig. 2a–c), with increasing rates of 8.3 mm/10yr, 1.1 mm/10yr, and 2.1 mm/10yr for the regions upstream of JM, MQ, and TNH, respectively. However, the trends are not statistically significant except for the basin upstream of JM. Insignificant precipitation changes during 1960–2006 were also suggested by Hu et al. (2012), who pointed out that annual precipitation changes over the SRYE were not noticeable except in the upper part of the region. The entire region shows a significant warming trend during 1961–2013 (Fig. 2d–f), with a mean warming rate of about 0.35 °C/10yr. Particularly, an accelerated warming is noticed for the recent 30 years across the SRYE. Differently from the changes in precipitation, yearly runoff shows a decreasing trend for all the three basins, although the trends are not statistically significant except for that at MQ (decrease by 9.2 mm/10yr). At JM and TNH, the runoff decreases by 3.2 mm/10yr and 6.0 mm/10yr, respectively.

4.2. Decadal variation

Strong decadal variations in climatic and hydrological variables over the SRYE have been suggested in previous studies, especially a significant decline of precipitation and discharge in the 1990s (Lan et al., 2010a; Zheng et al., 2009; Zhou and Huang, 2012). Fig. 3 shows variations in annual runoff, precipitation and mean temperature for the three basins, along with

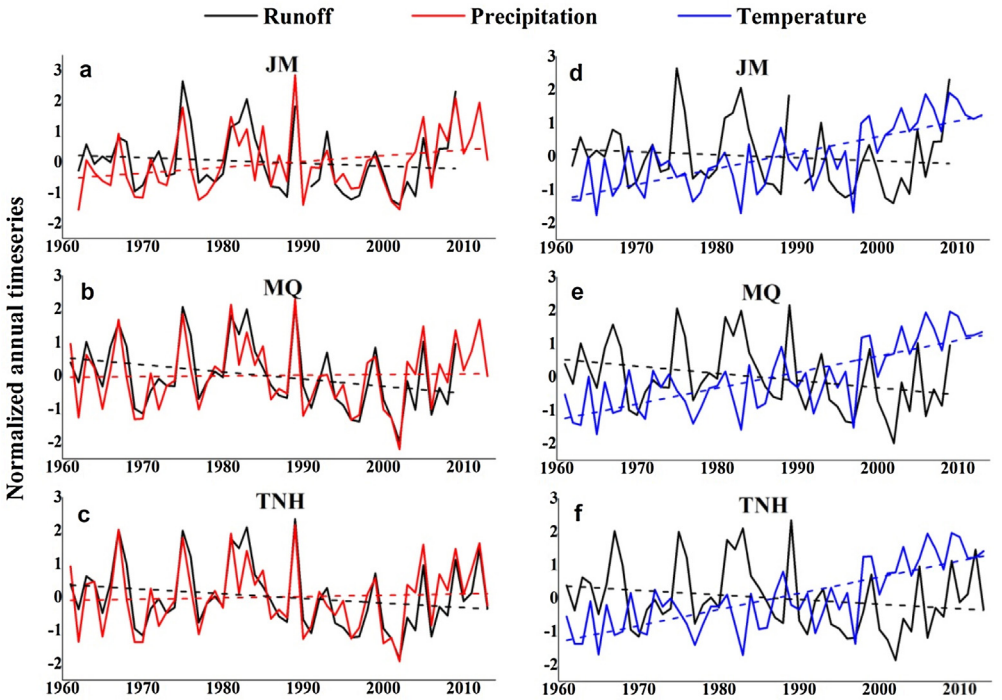

Fig. 2. Annual time series of normalized basin-averaged runoff, precipitation and temperature for the basins upstream of JM, MQ and TNH stations for the period 1961–2013. Dashed lines are the linear trends.

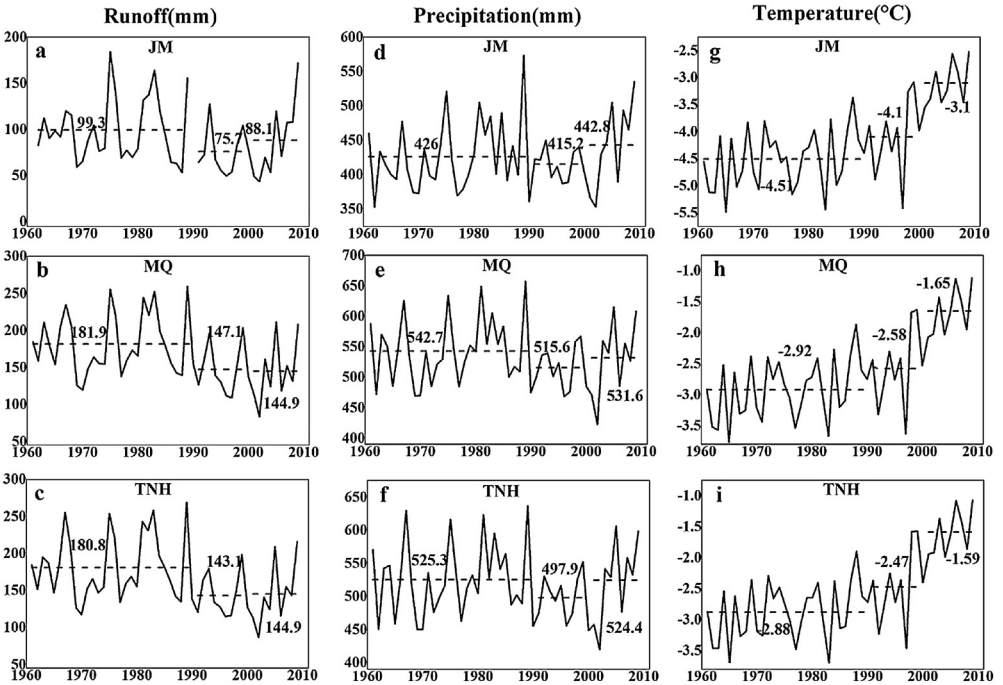

Fig. 3. Annual time series of basin-averaged runoff, precipitation and temperature for the three basins during 1961–2009. Means values for the reference period 1961–1990, and the periods 1990s and 2000s are also indicated.

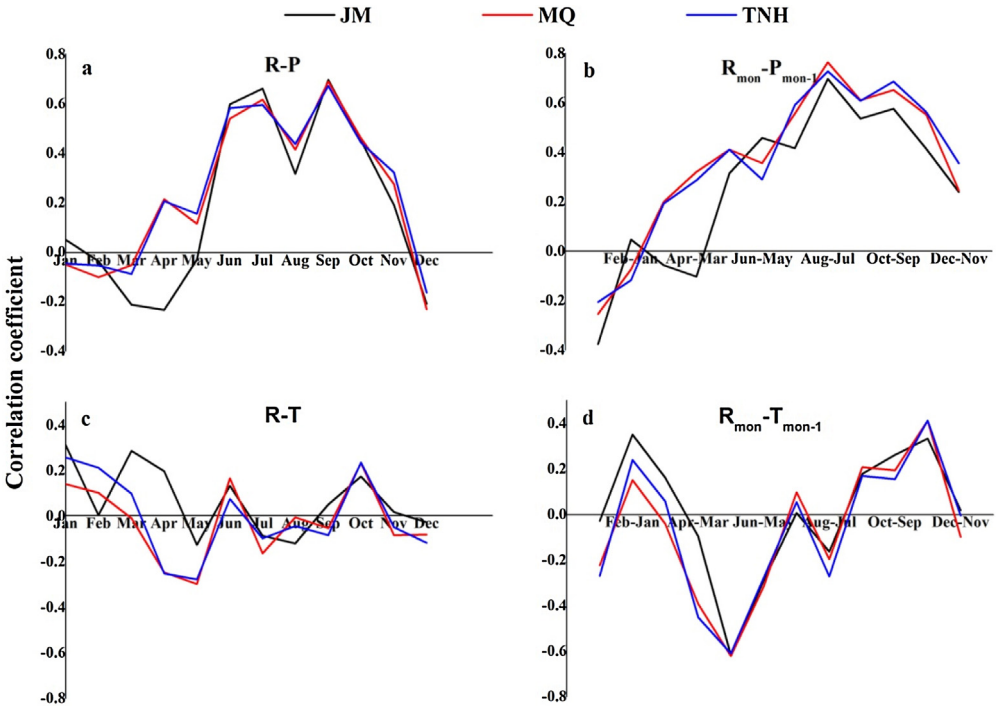

Fig. 4. Correlation coefficients between monthly runoff and precipitation (a, b) or temperature (c, d) for current month (a, c) and the relations between current month and previous month (b, d) over the three basins for 1961–2009.

the mean values for the periods 1961–1990, 1990s and 2000s. Among these three periods, the period 1961–1990 shows the highest runoff in all three basins; while the flow dramatically decreases in the 1990s (Fig. 3a–c) accompanied by a lower precipitation for all the basins (Fig. 3d–f). Precipitation rebounded in the 2000s and returned to a similar level as during the period 1961–1990. However, the runoff in the 2000s did not rebound to the level as in the reference period. At the same time, although precipitation in the 2000s was higher than that in the 1990s in all three basins, runoff was almost the same in the two periods except at JM with higher flows in the 2000s. A continuous warming was observed for all basins during 1961–2013 (Fig. 3g–i). This result is consistent with the Intergovernmental Panel on Climate Change (IPCC) fifth report, which reveals that each of the past three decades has a higher temperature than all the previous decades in the instrumental records (IPCC, 2013). Why runoff did not recover during the 2000s at the MQ and TNH stations along with the recovered precipitation relative to the period 1961–1990, Zhou and Huang (2012) explained that the increase in precipitation mostly occurred in the dry region of the SRYE where precipitation is mostly evaporated. We will further discuss and quantify the impacts of precipitation and temperature changes on runoff over the SRYE in Section 5.2.

4.3. Linkage between runoff and climate variables

Through a correlation analysis, the normalized annual time series of precipitation, temperature, and runoff (Fig. 2) reveal that the inter-annual runoff variations are highly consistent with the precipitation fluctuations (Fig. 2a–c), with correlation coefficients r of 0.75, 0.86 and 0.85 at the JM, MQ and TNH, respectively (significant at 10% level). The relationship between runoff and temperature is negative, less strong and insignificant (Fig. 2d–f). The good correspondence between runoff and precipitation variations suggests that precipitation plays a dominant role in the runoff generation over the SRYE.

Fig. 4 shows correlations between monthly runoff and precipitation/temperature with lags from 0 to 1 month. There is a significant positive relationship between precipitation and runoff during June–October for all the basins (r values of 0.32–0.70), with the highest correlations in June, July and September, and the lowest one in August (Fig. 4a). The strong correlations last from summer to November at MQ and TNH (r values of 0.27 and 0.36). Fig. 4b exhibits the correlations between runoff and precipitation in the previous month. R and P_{mon-1} are positively correlated significantly from May to November at JM, while it lasts from April to December at MQ and TNH. The r values are higher in August, October and November than those with a zero lag, suggesting that runoff is influenced by precipitation not only in current month but also previous month due to the delay of flow traveling downstream. It was also noticed that the r values between R and P_{mon-1} at MQ and TNH are generally larger than those for JM during April–November (Fig. 4b), indicating that the concentration time of streamflow close to the monthly scale considered for precipitation is higher downstream than upstream.

In the basin upstream of JM, runoff and temperature in the previous month are negatively correlated during May–June (Fig. 4d). Runoff and temperature tend to be negatively correlated at MQ and TNH, especially during April–May (Fig. 4c).

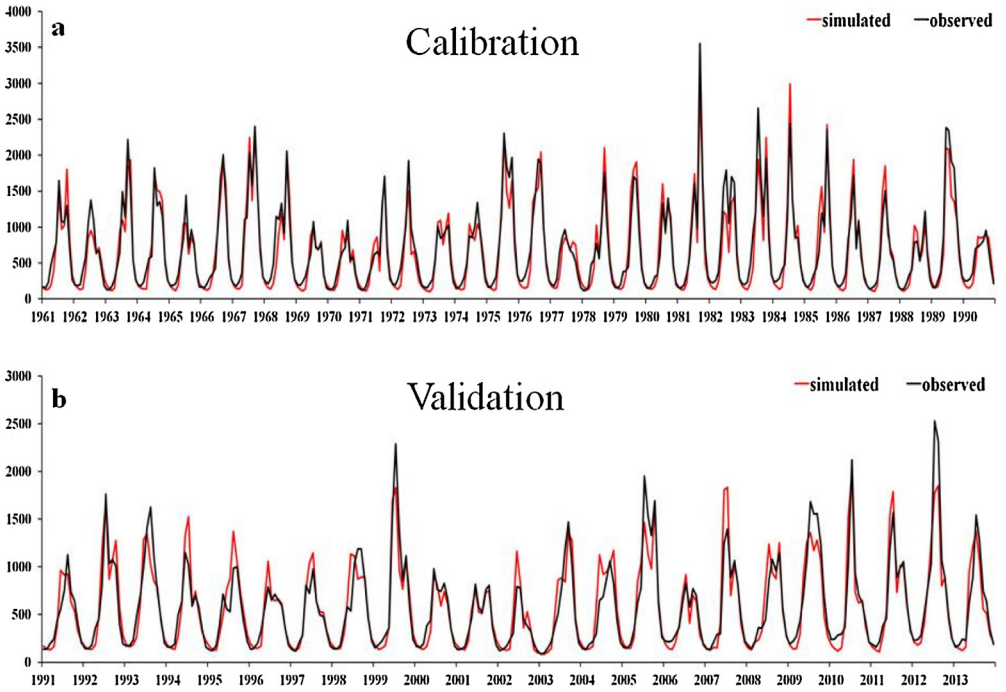

Fig. 5. Monthly time series of simulated and observed streamflow for the SRYE at TNH station during the calibration period 1961–1990 (a) and the validation period 1991–2013 (b).

Strong negative relationship also exists between R and $T_{mon\text{-}1}$ during April–Jun for MQ and TNH (negative r values in the range 0.31–0.62) (Fig. 4d). The reason why runoff is negatively correlated with temperature during spring and early summer is still unknown. A significant positive relationship between R and $T_{mon\text{-}1}$ in November is observed, with r values in the range 0.33–0.41 (Fig. 4d) for all basins. The strong positive relations between runoff and temperature in the autumn may suggest a fast melt of snowfall to produce runoff in this period. The modeling results in Zhang et al. (2013) also suggested a snowfall runoff peak in October over the SRYE.

5. Hydrologic impacts of meteorological changes

The correlation analysis in Section 4.3 has suggested a dominant role of precipitation in runoff generation over the SRYE. However, the overall decreasing runoff trend over the study period was accompanied by an overall long-term increasing trend in precipitation (Fig. 2). This result may imply that other factors also affect flow variations. On the decadal time scales (Fig. 3), precipitation in the 2000s was 3.1% and 5.3% higher than that in the 1990s for MQ and TNH, whereas runoff was almost the same in these two time periods (Fig. 3b–c). This may suggest a reduction in runoff generation. The increase in evapotranspiration in a rapidly warming climate may be the reason. Since actual evapotranspiration observations with long-term records at large scales are not available in the SRYE, we quantified the evapotranspiration changes in both time and space with the VIC land surface model. The VIC model was evaluated through comparisons between simulated and observed streamflow at the TNH station.

5.1. Calibration and validation of hydrological model

Fig. 5 presents monthly time series of simulated and observed streamflow at the TNH station during 1961–2013. Regarding the use of the hydrological model for simulating runoff changes due to changes in meteorological conditions, we split the study period into calibration period (1961–1990) and validation period (1991–2013). The VIC model simulations captured the variations and magnitude of streamflow well during both the calibration and validation periods (Fig. 5), with the Nash-Sutcliffe efficiency (E_{NS}) and relative error (Er) values of 0.90, and −1.4%, respectively in the calibration period and 0.84 and 2.8% in the validation period. This performance can be classified as good for the calibration period and satisfactory for the validation period following the ratings in Table 1.

To further investigate the reliability of the VIC simulated actual evapotranspiration, we compared the GRACE-derived evapotranspiration (Eq. (1)) with the VIC estimates (Fig. 6). The correlation coefficient between them is 0.75 and the Er is −1.1%. Given that the GRACE method is completely independent from the VIC model, the good agreement between both

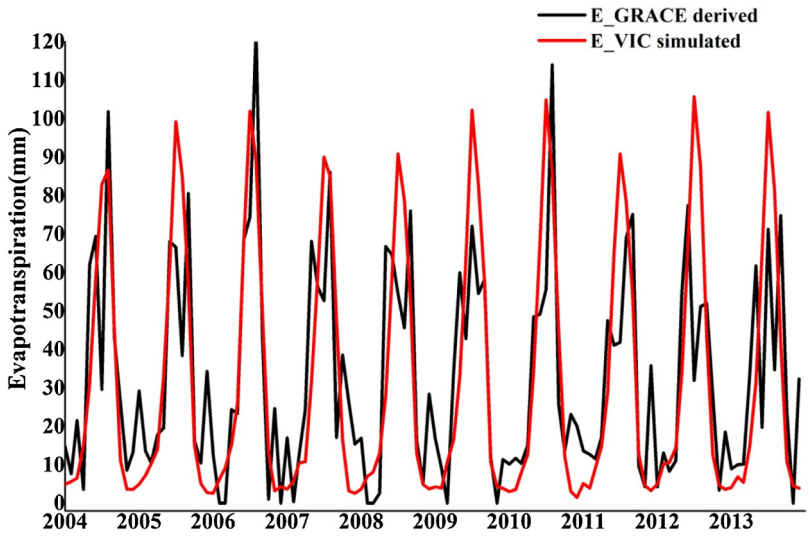

Fig. 6. Estimates of monthly actual evapotranspiration from the VIC model and GRACE data for 2004–2013.

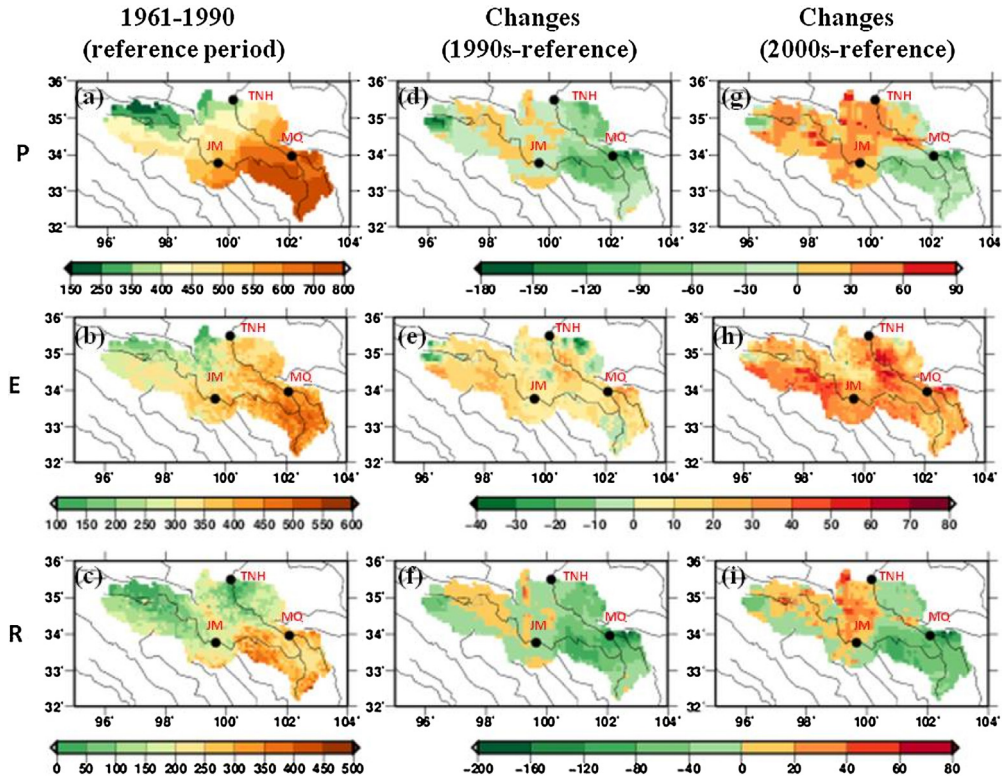

Fig. 7. Spatial distribution of mean annual precipitation, evapotranspiration and runoff in the reference period 1961–1990 (a–c), and their changes in the 1990s (d–f) and 2000s (g–i) relative to the reference period.

actual evapotranspiration estimates suggests that the VIC simulated ET is reasonable and can be used to quantify the ET changes over the SRYE.

5.2. Meteorological change impacts on annual runoff

Based on the calibrated VIC model, we investigated the spatial changes of precipitation, runoff and actual evapotranspiration in response to the meteorological changes and variations over the SRYE. Fig. 7 presents the spatial distribution of mean annual precipitation, actual evapotranspiration and runoff for the reference period 1961–1990, and their changes in

Table 2
Precipitation (P), runoff (R) and evapotranspiration (ET) changes in the 1990s and 2000s compared with the reference period 1961–1990 for JM, JM-MQ, MQ-TNH and the entire SRYE.

		JM	JM-MQ	MQ-TNH	TNH
P	1961–1990	427.1	682.5	482.3	525.3
	1991–2000	415.2(−2.8%)	635.4(−6.9%)	454.4(−5.8%)	497.9(−5.2%)
	2001–2009	442.8(3.7%)	637.6(−6.6%)	506.6(5.1%)	524.4(−0.2%)
R	1961–1990	99.3	274.3	178.2	180.8
	1991–2000	75.7(−23.8%)	225.4(−17.8%)	133.8(−24.9%)	143.1(−20.8%)
	2001–2009	88.1(−11.3%)	207.2 (−24.5%)	144.8(−18.7%	144.9(−19.9%)
ET	1961–1990	294.8	417.9	328.1	344.3
	1991–2000	307.1(4.2%)	425.6(1.8%)	333.8(1.7%)	352.2(2.3%)
	2001–2009	320.4(8.7%)	441.6(5.7%)	352.6(7.5%)	369(7.1%)

Table 3
Contribution of precipitation and evapotranspiration to runoff changes in the 1990s and 2000s.

	Time	Formula	Contribution	
			P	E
JM	1991–2000	$-23.8 = 4 \times (-2.8) + (-3) \times 4.2$	47%	53%
	2001–2009	$-11.3 = 4 \times 3.7 + (-3) \times 8.7$		100%
JM-MQ	1991–2000	$-17.8 = 2.09 \times (-6.9) + (-1.88) \times 1.8$	81%	19%
	2001–2009	$-24.5 = 2.09 \times (-6.6) + (-1.88) \times 5.7$	56%	44%
MQ-TNH	1991–2000	$-24.9 = 2.97 \times (-5.8) + (-4.51) \times 1.7$	69%	31%
	2001–2009	$-18.7 = 2.97 \times 5.1 + (-4.51) \times 7.5$		100%
TNH	1991–2000	$-20.8 = 2.8 \times (-5.2) + (-2.72) \times 2.3$	70%	30%
	2001–2009	$-19.9 = 2.8 \times (-0.2) + (-2.72) \times 7.1$	3%	97%

the 1990s and 2000s relative to the reference period. The data show the highest annual precipitation in the southeast of the SRYE, with a mean annual value of about 700–800 mm, and decreasing towards the northwest, with annual precipitation as low as 150–250 mm in the very upstream parts of the SRYE (Fig. 7a). The spatial patterns of actual evapotranspiration and runoff (Fig. 7b and c) generally follow that of precipitation, with the highest evapotranspiration and runoff in the southeast of the basin where there is sufficient water for evaporation. The region JM-MQ (Fig. 7c) in the southeast is also the major runoff generation area (annual R of 300–500 mm) in the SRYE. The driest area is in the upstream region of JM (annual R < 150 mm) and the very downstream parts of the SRYE (Fig. 7c).

Precipitation consistently decreased almost over the entire basin in the 1990s (Fig. 7d) by 2.8–6.9% relative to the reference period over the three sub-regions (Table 2). The spatial pattern of runoff changes in the 1990s is similar to that of precipitation (Fig. 7f), but with a stronger decrease of 20.8% (Table 2). However, actual evapotranspiration shows positive changes in the 1990s (Fig. 7e), with a mean increase of 2.3% (Table 2), which is consistent with the continuous warming in the 1990s (Fig. 3). Therefore, the decrease in precipitation and increase in evapotranspiration both contributed to the runoff decrease in the 1990s. In the 2000s, precipitation (Fig. 7g) exhibited inhomogeneous change over the basin, with an increase in the upstream regions of JM (3.7%) and MQ-TNH (5.1%), opposed to a decrease in the major runoff generation area for JM-MQ (6.6%). Despite these changes, precipitation almost stayed unchanged for the basin as a whole (Table 2). In the 2000s, the pattern of runoff changes differed from that of precipitation (Fig. 7g and i). Runoff decreased in the upstream parts of JM and MQ-TNH (11.3–18.9%) while precipitation increased, and the runoff decreased even more in the region JM-MQ (24.5%), leading to a mean decrease in runoff by nearly 20% over the entire SRYE. Along with the rapid warming in the 2000s (Fig. 3), evapotranspiration largely increased in the 2000s (Fig. 7h) relative to the reference period (mean increase of 7.1%; Table 2). Results in Fig. 7 and Table 2 also suggest that the runoff changes in the 1990s and 2000s over the SRYE are the result of both precipitation and evapotranspiration changes associated with the warming climate. However, what is the contribution of each meteorological variable to the runoff changes over the SRYE?

To answer the question on the contribution of each meteorological variable to the runoff changes, we computed the climate elasticity based on the runoff and meteorological changes in the 1990s and 2000s relative to 1961–2000 (Table 3). The elasticity of runoff in relation to precipitation and evapotranspiration are 2.8 and −2.72 over the SRYE, respectively, meaning that 1% increase of precipitation results in 2.8% increase of runoff, while 1% increase of evapotranspiration leads to 2.72% decrease of runoff. In the 1990s, evapotranspiration and precipitation played a similar role in the runoff changes for JM, while precipitation exhibited a more important role in runoff reduction for the sub-basins between JM and TNH (69–81%; Table 3). On average, evapotranspiration increase accounted for 30% of the runoff decrease in the SRYE in the 1990s (Table 3). During the 2000s, the contribution of evapotranspiration (44–100%; Table 3) to runoff changes increased in all the basins relative to the 1990s. For the JM and MQ-TNH basins, the runoff reduction can be entirely attributed to the evapotranspiration increase (Table 2, Table 3). For the major runoff generation area JM-MQ, precipitation still exerted an important role in the runoff changes in the 2000s, with a contribution of 56% (Table 3), a little bit higher than the influence

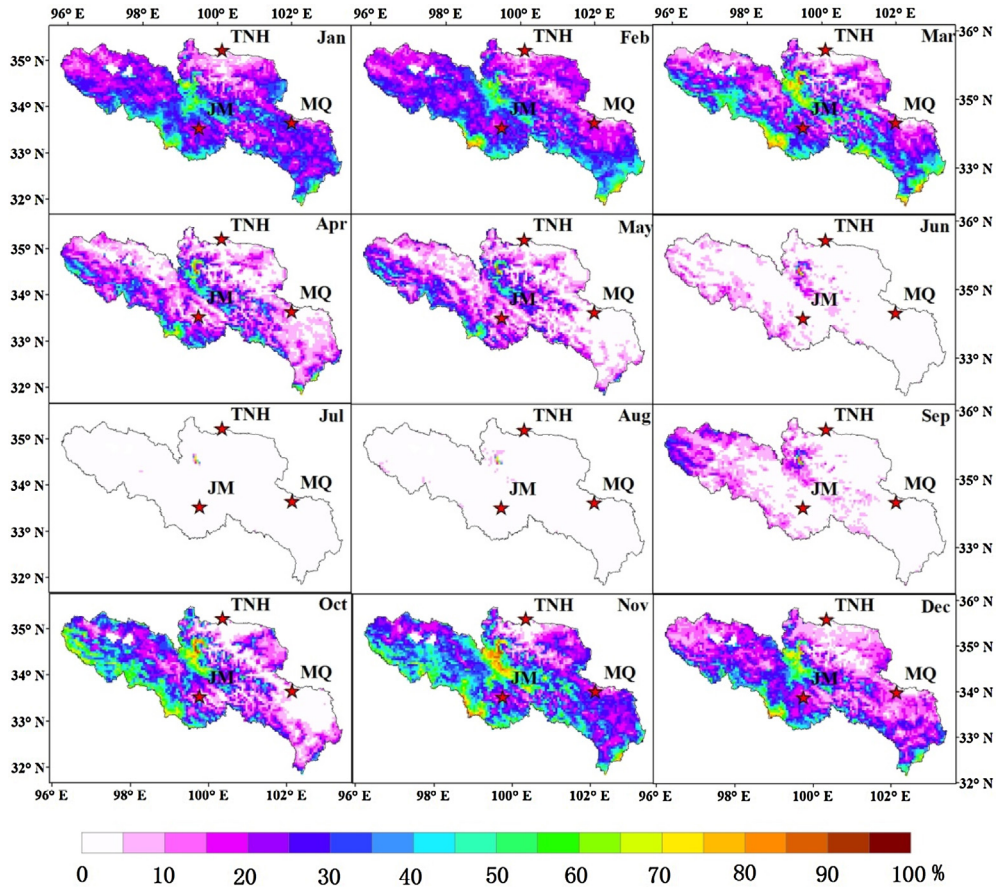

Fig. 8. Spatial distribution of mean monthly snow coverage (%) in the SRYE for 2001–2012.

of evapotranspiration (44%; Table 3). For the basin average, evapotranspiration contributed 97% of the runoff changes in the 2000s (Table 3), suggesting that the influence of evapotranspiration on the runoff is increasing along with the increased warming over the SRYE. This may partly explain the reason why precipitation recovered to the level of 1960–1990 in the 2000s but runoff was still low (Fig. 3). The increased precipitation in JM and MQ-TNH mostly evaporated due to the rapid warming in the 2000s. Another reason was that precipitation decreased in the major runoff generation area JM-MQ in the 2000s, resulting in a larger runoff decrease accompanied with the increased evapotranspiration (5.7%; Table 2).

5.3. Meteorological change impacts on seasonal snow cover and spring flow

The SRYE is extensively covered by snow with a mean annual coverage of about 18% based on the MOD10C2 data during 2001–2012 (Fig. 8). The region upstream of JM has the most extensive snow cover, with mean annual coverage of about 21%, while the JM-MQ (16%) and MQ-TNH (14%) areas have relatively smaller coverage. The snowpack begins to accumulate in October, with the highest concentration in the southeast of the upstream basins and the Anyemaqen mountains (Fig. 8). The snow cover starts to melt in April and May, and mostly melts away in June except for the Anyemaqen Mountains. We examined the trends of snow cover for each month during 2001–2012 and found that it decreased for all the basins in May by 1.1–1.3%/yr (Fig. 9a). Fig. 9b–d present the normalized variations of temperature and snow cover in May during 2001–2012 for the three basins. The temperature in May exhibits a warming trend during 2001–2012 and is negatively correlated with the snow cover variations (Fig. 9b–d), with high correlation coefficients of −0.7 at JM, −0.8 at MQ and −0.85 at TNH.

Results in Fig. 9b–d suggest that the decrease in May snow cover might be associated with the climate warming which may further affect spring streamflow due to snow melt. Fig. 10b–d show the mean daily streamflow at the three stations JM, MQ and TNH during the spring time (March–May) in the 1980s, 1990s and 2000s. A spring peak flow caused by spring snow melt appeared in late April to early May at JM. It is clearly seen that the spring peak flow at JM tends to occur earlier in the past three decades (Fig. 10b). In the 1980s, the peak occurred on May 12, whereas it happened on May 4 in the 1990s and on April 27 in the 2000s. In the past 30 years, the timing of spring peak advanced by about 15 days at JM. This earlier shift can be explained by the earlier sn$ow melt due to the enhanced warming. Fig. 10a exhibits the April temperature of each decade at JM. The temperature was about the same in the 1960s and 1970s, while it showed a warming trend during

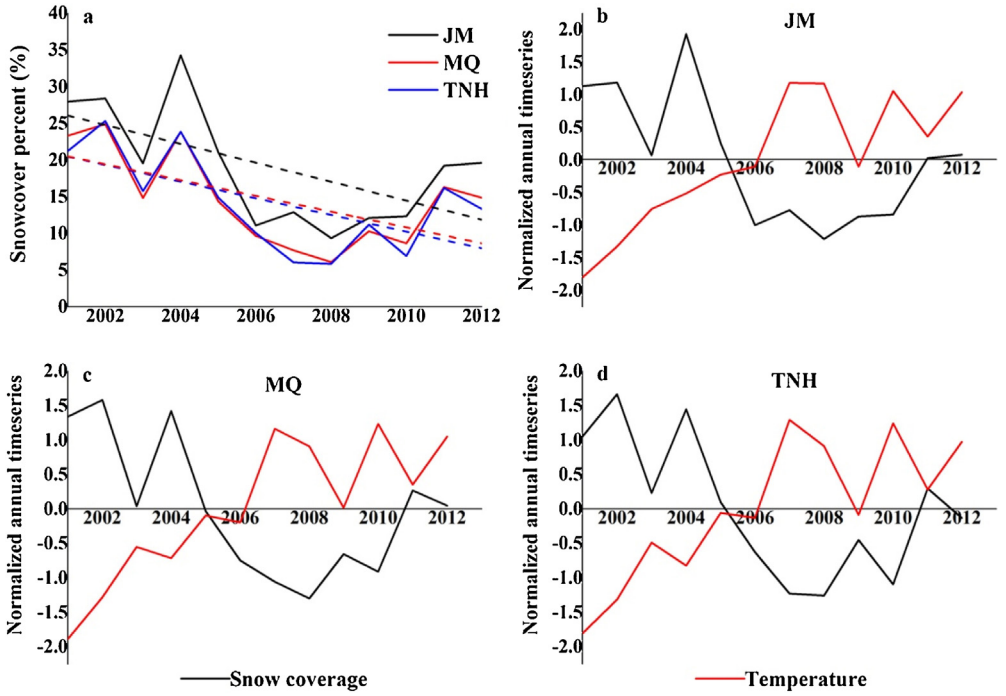

Fig. 9. Trends of snow coverage in May in the basins upstream of JM, MQ and TNH (a), and normalized snow coverage and temperature in May during 2001–2012 in the three basins (b–d).

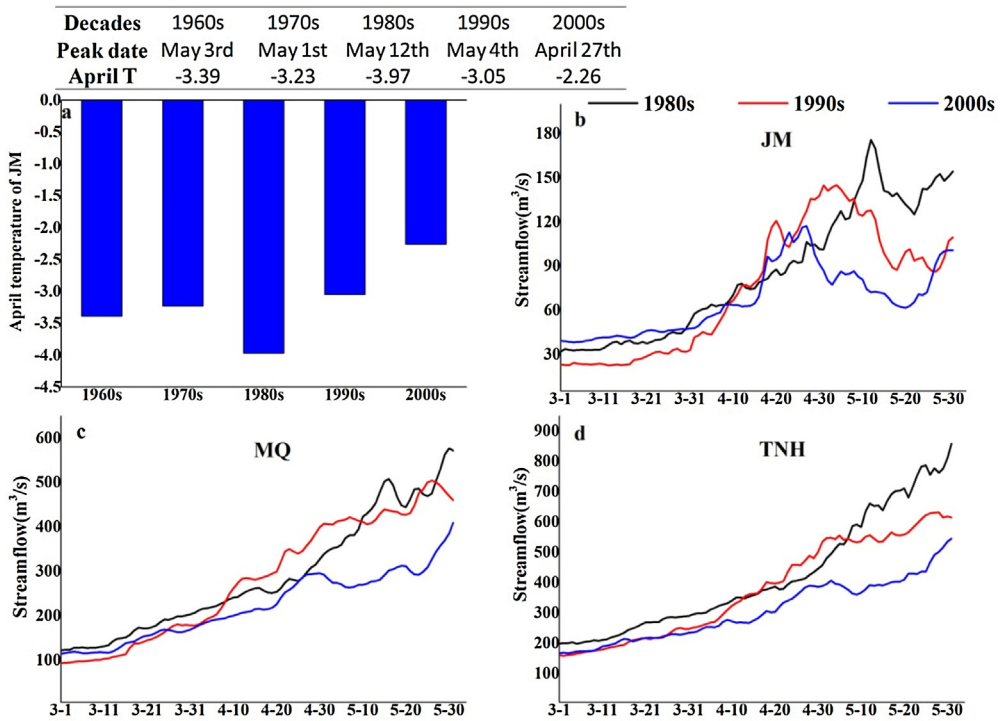

Fig. 10. Mean temperature of April in 5 decades at JM (a), mean daily streamflow at JM, MQ and TNH during March–May in the 1980s, 1990s and 2000s (b–d).

the 1980s–2000s, consistent with the shift of spring peak flows at JM. For MQ and TNH (Fig. 10c–d), the spring flow rises more smoothly than at JM and seldom has clear sharp peaks during March–May. This is probably because the MQ and TNH areas have less snow coverage and the rainfall runoff plays a more important role in the spring and summer runoff flows of downstream areas.

6. Discussion

Our analyses suggest that, in the 1990s, runoff changes over the SRYE were caused by both decrease in precipitation and increase in evapotranspiration, with the decrease in precipitation playing a dominate role. In the 2000s, runoff changes were mainly caused by the increase in evapotranspiration especially in the dry regions upstream of JM and MQ-TNH (runoff ratios of 0.21–0.34). The wide spread of lakes and wetlands at JM may favor the increase in evapotranspiration along with climate warming. In this work, we only took meteorological changes and variations into consideration, while the impacts of land cover changes on runoff were not analyzed because the SRYE less affected by human activities (Cuo et al., 2013, 2015). Cuo et al. (2013), through a modeling approach, reported that the runoff changes upstream of TNH during the past few decades were mostly caused by meteorological changes, and the impacts of land cover changes on runoff changes were very small. However, Zheng et al. (2009), using a climate elasticity approach, estimated that the land cover changes contributed for more than 70% to the runoff reduction in the 1990s. The inconsistencies between our and their conclusions may be partly caused by the different approaches used. Studies in other basins in the Tibetan Plateau suggested that land cover change and human activities such as surface water and groundwater exploitation, new water-related policy implementation, agricultural production activities may exert great influence on runoff changes (Zhang et al., 2015; Pervez and Henebry, 2015; Huo et al., 2008). In fact, in a warming climate, the SRYE is undergoing great changes, such as wetland and frozen soil changes, as well as lakes expansion, which may result in land cover changes. The grassland area after 1990 decreased by about 10% relative to the previous years, and the sandy land increased by around 4% over the SRYE (Zheng et al., 2009). Limited by the harsh living conditions, the population size is small in this region. The urbanization and industrialization are very slow as well, thus water abstractions have not changed too much. While the number of livestock increased threefold during 1970–2000 in the area upstream of HHY (Wang et al., 2000), water abstractions for livestock certainly increased. Meanwhile, a hydropower 17 Km downstream of Eling lake was build in 1998 and in operation since 2001. To what extent these changes and human activities are responsible for the decreasing runoff should be considered in the future work.

There are extensive frozen soils in the SRYE, which is essential to preserve the water resources (Li et al., 2012). Along with the warming climate, many studies have suggested that the TP is experiencing permafrost degradation (Cheng and Jin, 2012; Cheng and Wu, 2007; Wu et al., 2007). The increase in active layer thickness of permafrost due to warmer temperature leads to more water for evaporation and hence reduced runoff. At the same time, the gradually thicken active layer may hold more water in the soil layers and lead to less surface runoff. Although it is accepted that climate change is one of the major drivers for hydrological changes, the effects of permafrost degradation on runoff processes still remain controversial. Thus, further research is needed to explore to what extent permafrost degradation might impact runoff changes over the SRYE. In the complex background of environment changes including climate change, land cover changes, frozen soil degradation and human activities, soil moisture and groundwater may also change, thus leading to different conditions of runoff generation.

The long-term linear trends of precipitation, runoff and temperature (Fig. 2) present a general temporal change of these variables in the past 50 years. However, given the relatively short records, these also might be the influence of inter-annual and decadal variability (Fig. 3) (Hannaford et al., 2013; Willems, 2013b). Fig. 2 clearly exhibited decadal variations in runoff and precipitation. As shown by Willems (2013a) and Taye and Willems (2013) and others for other regions in the world, the decadal variations might be explained by atmospheric or oceanographic oscillations such as El Niño southern oscillation (ENSO), the Pacific Decadal Oscillation (PDO), the Southern Oscillation Index (SOI), the North Atlantic Oscillation (NAO), and the Atlantic Multidecadal Oscillation (AMO). A study in the Blue Nile river basin in East Africa showed that multi-decadal oscillations modulated the high streamflows and that the influence of watershed characteristics changes is very small (Taye et al., 2015). In the SRYE, the temporal changes in runoff appear explained by both long-term trends and decadal variations of climate.

Annual runoff and annual mean temperature were found negatively correlated over the SRYE during 1961–2009, which is consistent with the finding of the climate sensitivity analysis with the VIC model, which showed that the increase in evapotranspiration along with the warming climate was the main factor for runoff decrease in the 2000s. At the annual scale, the negative correlation between runoff and temperature was not significant. This is different at monthly scale, where significant negative correlation was found during March to June (Fig. 4c and d). In these months, the evapotranspiration may increase due to the warming temperature, explains the drop in streamflow. In the wet season (July–September), there was no significant relationship between temperature and precipitation, because precipitation was quite high, and temperature had a relatively small effect on the runoff changes. In spring and late summer, precipitation is not that high as in the wet season, thus its effect on runoff is very weak, and the role of temperature on runoff is bigger relative to precipitation. This may explain why runoff and temperature are not significantly correlated at annual scales.

The sensitivity analysis in this work assumed that runoff changes solely result from meteorological changes (precipitation and evapotranspiration), and that their contributions to runoff changes are independent. However, precipitation impacts evapotranspiration indirectly through soil moisture. This effect was considered secondary and neglected, but needs further investigation. Also further validation of the VIC model may be useful, in order to test the validity of the model to accurately

simulate changes in runoff as a result of meteorological changes beyond the range of meteorological conditions considered during the standard model calibration and validation as considered in this study; see Refsgaard et al. (2014) and Van Steenbergen and Willems (2012) for potential methods.

7. Conclusions

In this work, we have investigated the spatial-temporal changes of hydrological and meteorological variables and the linkage between runoff and precipitation/temperature over the SRYE during 1961–2013. The impacts of precipitation and temperature on the hydrological changes were quantified through climate elasticity by applying the VIC land surface hydrological model. The impacts of the warming climate on the seasonal snow cover and spring streamflow over the SRYE were also examined. The main findings of this study are as below:

(1) During the period 1961–2013, annual precipitation over the SRYE exhibited weakly increasing trends, while the precipitation upstream of JM increased significantly by about 8.3 mm/10yr. Temperature showed consistently warming trends in all the basins of the SRYE with a mean warming rate of 0.35 °C/10yr. Meanwhile, runoff decreased at the three hydrological stations by about 3.2 mm/10yr, 9.2 mm/10yr and 6.0 mm/10yr at the JM, MQ and TNH stations, respectively.
(2) Relative to the reference period 1961–1990, runoff decreased by about 21% in the 1990s over the SRYE. The decrease in precipitation and the weak increase in evapotranspiration both contributed to the runoff drop in the 1990s. However, decrease in precipitation played a more important role (70%) than increase in evapotranspiration (30%) in this runoff reduction. Runoff decreased by about 20% in the 2000s, during which precipitation contributed for 3% to the runoff reduction, while the increase in evapotranspiration accounted for 97%. Due to strong warming over the SRYE, evapotranspiration is playing an increasingly important role in affecting runoff changes in recent decades.
(3) Analysis of the MODIS data show a decreased trend of snow cover in May over the SRYE during 2001–2012; this change was closely related to the strong warming temperature in the past decade. In the past 30 years, the spring peak flow mainly caused by snowmelt occurred earlier for about 15 days at the JM station. This shift in peak flow timing is expected to be due to an earlier snow melting associated with the climate warming over the SRYE.

Conflict of interest

Due to the conflict of interest, we would suggest avoid the potential reviewers from the same institute as the first and corresponding authors-the Institute of Tibetan Plateau Research, CAS.

Acknowledgments

We thank Prof. Zhongbo Yu for his helpful comments. This work was supported by the National Natural Science Foundation of China (41190081, 41171051) and the “Strategic Priority Research Program (B)” of the Chinese Academy of Sciences (XDB03030209).

Appendix A. Supplementary data

Supplementary data associated with this article can be found, in the online version, at http://dx.doi.org/10.1016/j.ejrh.2016.03.003.

References

Barnett, T.P., Adam, J.C., Lettenmaier, D.P., 2005. Potential impacts of a warming climate on water availability in snow-dominated regions. Nature 438 (7066), 303–309, http://dx.doi.org/10.1038/nature04141.
Cai, X., Rosegrant, M.W., 2004. Optional water development strategies for the Yellow River basin: balancing agricultural and ecological water demands. Water Resour. Res. 40 (8), http://dx.doi.org/10.1029/2003wr002488, n/a–n/a.
Chen, L., Liu, C., Li, Y., Wang, G., 2007. Impacts of climatic factors on runoff coefficients in source regions of the Huanghe River. Chin. Geogr. Sci. 17 (1), 047–055, http://dx.doi.org/10.1007/s11769-007-0047-4.
Cheng, G., Jin, H., 2012. Permafrost and groundwater on the Qinghai-Tibet Plateau and in northeast China. Hydrol. J. 21 (1), 5–23, http://dx.doi.org/10.1007/s10040-012-0927-2.
Cheng, G., Wu, T., 2007. Responses of permafrost to climate change and their environmental significance, Qinghai-Tibet Plateau. J. Geophys. Res. 112 (F2), http://dx.doi.org/10.1029/2006jf000631.
Cherkauer, K.A., Lettenmaier, D.P., 2003. Simulation of spatial variability in snow and frozen soil. J. Geophys. Res. 108 (D22), 8858, http://dx.doi.org/10.1029/2003jd003575.
Cherkauer, K.A., Lettenmaier, D.P., 1999. Hydrologic effects of frozen soils in the upper Mississippi River basin. J. Geophys. Res. 104 (D16), 19599–19610.
Cuo, L., Zhang, Y., Gao, Y., Hao, Z., Cairang, L., 2013. The impacts of climate change and land cover/use transition on the hydrology in the upper Yellow River basin, China. J. Hydrol. 502, 37–52, http://dx.doi.org/10.1016/j.jhydrol.2013.08.003.
Cuo, L., Zhang, Y., Zhu, F., Liang, L., 2015. Characteristics and changes of streamflow on the Tibetan Plateau: a review. J. Hydrol.: Reg. Stud. 2, 49–68.
Dooge, J.C.I., Bruen, M., Parmentier, B., 1999. A simple model for estimating the sensitivity of runoff to long-term changes in precipitation without a change in vegetation. Adv. Water Resour. 23, 153–163, http://dx.doi.org/10.1016/S0309-1708(99)00019-6.
Fu, G., Chen, S., Liu, C.M., 2004. Hydro-climatic trends of the Yellow River basin for the last 50 years. Clim. Change 65, 149–178.
Fu, G., Charles, S.P., Chiew, F.H.S., 2007. A two-parameter climate elasticity of streamflow index to assess climate change effects on annual streamflow. Water Resour. Res. 43 (11), http://dx.doi.org/10.1029/2007wr005890, n/a–n/a.

Hannaford, J., Buys, G., Stahl, K., Tallaksen, L.M., 2013. The influence of decadal-scale variability on trends in long European streamflow records. Hydrol. Earth Syst. Sci. 17, 2717–2733.
Hansen, M., DeFries, R., Townshend, J.R.G., Sohlberg, R., 2000. Global land cover classification at 1 km resolution using a decision tree classifier. Int. J. Remote Sens. 21, 1331–1365.
Hu, Y., Maskey, S., Uhlenbrook, S., Zhao, H., 2011. Streamflow trends and climate linkages in the source region of the Yellow River, China. Hydrol. Process. 25 (22), 3399–3411, http://dx.doi.org/10.1002/hyp.8069.
Hu, Y., Maskey, S., Uhlenbrook, S., 2012. Trends in temperature and rainfall extremes in the Yellow River source region, China. Clim. Change 110 (1–2), 403–429, http://dx.doi.org/10.1007/s10584-011-0056-2.
Huo, Z., Feng, S., Kang, S., Li, W., Chen, S., 2008. Effects of climate changes and water-related human activities on annual streamflows of the Shiyang River basin in arid north-west China. Hydrol. Process. 22, 3155–3167.
IPCC AR5, 2013. Climate change 2013: The physical science basis, in Contribution of Working Group I (WGI) to the Fifth Assessment Report (AR5) of the Intergovernmental Panel on Climate Change (IPCC).
Lan, Y., Kang, E., Ma, Q., Yang, W., Yao, Z., 1999. Runoff forecast model for inflow to the longyangxia reservoir in the Upper Yellow River basin during spring. J. Glaciol. Geocryol. 21 (4), 391–395.
Lan, Y., et al., 2010a. Response of runoff in the headwater region of the Yellow River to climate change and its sensitivity analysis. J. Geogr. Sci. 20 (6), 848–860, http://dx.doi.org/10.1007/s11442-010-0815-4.
Lan, Y., et al., 2010b. Response of runoff in the source region of the Yellow River to climate warming. Quat. Int. 226 (1–2), 60–65, http://dx.doi.org/10.1016/j.quaint.2010.03.006.
Li, L., Shen, H., Dai, S., Xiao, J., Shi, X., 2012. Response of runoff to climate change and its future tendency in the source region of Yellow River. J. Geogr. Sci. 22 (3), 431–440, http://dx.doi.org/10.1007/s11442-012-0937-y.
Li, Z., Liu, X., Ma, T., Kejia, D., Zhou, Q., Yao, B., Niu, T., 2013. Retrieval of the surface evapotranspiration patterns in the alpine grassland–wetland ecosystem applying SEBAL model in the source region of the Yellow River, China. Ecol. Modell. 270, 64–75, http://dx.doi.org/10.1016/j.ecolmodel.2013.09.004.
Liang, X., Lettenmaier, D.P., Wood, E.F., Burges, S.J., 1994. A simple hydrologically based model of land surface water and energy fluxes for general circulation models. J. Geophys. Res. 99 (D17), 14415–14428.
Liang, X., Wood, E.F., Lettenmaier, D.P., 1996. Surface soil moisture parameterization of the VIC-2 L model: evaluation and modification. Glob. Planet. Change 13, 195–206.
Liu, X., Liu, C., Luo, Y., Zhang, M., Xia, J., 2012. Dramatic decrease in streamflow from the headwater source in the central route of China's water diversion project: climatic variation or human influence? J. Geophys. Res. D. Atmos. 117 (D6), http://dx.doi.org/10.1029/2011jd016879.
Lohmann, D., Raschke, E., Nijssen, B., Lettenmaier, D.P., 1998. Regional scale hydrology: I. Formulation of the VIC-2L model coupled to a routing model. Hydrol. Sci. J. 43 (1), 131–141, http://dx.doi.org/10.1080/02626669809492107.
Lu, A., Jia, S., Yan, H., Yang, G., 2009. Temporal variations and trend analysis of the snow melt runoff timing across the source regions of the Yangtze River, Yellow River and Lancang River. Resour. Sci. 31 (10), 1704–1709 (in Chinese with English abstract).
Moriasi, D.N., Arnold, J.G., Van Liew, M.W., Bingner, R.L., Harmel, R.D., Veith, T.L., 2007. Model evaluation guidelines for systematic quantification of accuracy in watershed simulations. Trans. ASABE 50, 885–900.
Morrow, E., Mitrovica, J.X., Fotopoulos, G., 2011. Water storage, net precipitation, and evapotranspiration in the mackenzie river basin from october 2002 to september 2009 inferred from GRACE satellite gravity data. J. Hydrometeorol. 12 (3), 467–473, http://dx.doi.org/10.1175/2010jhm1278.1.
Nash, J.E., Sutcliffe, J.V., 1970. River flow forecasting through conceptual models part I—a discussion of principles. J. Hydrol. 10 (3), 282–290.
Pervez, M.S., Henebry, G.M., 2015. Assessing the impacts of climate and land use and land cover change on the freshwater availability in the Brahmaputra River basin. J. Hydrol.: Reg. Stud. 3, 285–311.
Qin, D.H., Liu, S.Y., Li, P.J., 2006. Snow cover distribution, variability, and response to climate change in western China. J. Clim. 19 (9), 1820–1833.
Ramillien, G., Frappart, F., Güntner, A., Ngo-Duc, T., Cazenave, A., Laval, K., 2006. Time variations of the regional evapotranspiration rate from Gravity Recovery and Climate Experiment (GRACE) satellite gravimetry. Water Resour. Res. 42 (10), http://dx.doi.org/10.1029/2005wr004331, n/a–n/a.
Refsgaard, J.C., Madsen, H., Andréassian, V., Arnbjerg-Nielsen, K., Davidson, T.A., Drews, M., Hamilton, D., Jeppesen, E., Kjellström, E., Olesen, J.E., Sonnenborg, T.O., Trolle, D., Willems, P., Christensen, J.H., 2014. A framework for testing the ability of models to project climate change and its impacts. Clim. Change 122, 271–282.
Rodell, M., Famiglietti, J.S., Chen, J., Seneviratne, S.I., Viterbo, P., Holl, S., Wilson, C.R., 2004. Basin scale estimates of evapotranspiration using GRACE and other observations. Geophys. Res. Lett. 31 (20), http://dx.doi.org/10.1029/2004gl020873.
Sankarasubramanian, A., Vogel, R.M., Limbrunner, J.F., 2001. Climate elasticity of streamflow in the United States. Water Resour. Res. 37 (6), 1771–1781, http://dx.doi.org/10.1029/2000WR900330.
Sato, Y., Ma, X., Xu, J., Matsuoka, M., Zheng, H., Liu, C., Fukushima, Y., 2008. Analysis of long-term water balance in the source area of the Yellow River basin. Hydrol. Process. 22 (11), 1618–1629, http://dx.doi.org/10.1002/hyp.6730.
Schaake, J.C., 1990. In: Waggoner, P.E. (Ed.), From Climate to Flow, in Climate Change and U.S. Water Resources. John Wiley, New York, pp. 177–206 (chapter 8).
Stewart, I.T., 2009. Changes in snowpack and snowmelt runoff for key mountain regions. Hydrol. Process. 23 (1), 78–94, http://dx.doi.org/10.1002/hyp.7128.
Storck, P., Lettenmaier, D.P., 1999. Predicting the effect of a forest canopy on ground snow accumulation and ablation in maritime climates. In: Troendle, C. (Ed.), 67th Western Snow Conference. Colo. State Univ, pp. 1–12.
Swenson, S., Yeh, P.J.F., Wahr, J., Famiglietti, J., 2006. A comparison of terrestrial water storage variations from GRACE with in situ measurements from Illinois. Geophys. Res. Lett. 33 (16), http://dx.doi.org/10.1029/2006gl026962.
Syed, T.H., Famiglietti, J.S., Rodell, M., Chen, J., Wilson, C.R., 2008. Analysis of terrestrial water storage changes from GRACE and GLDAS. Water Resour. Res. 44 (2), http://dx.doi.org/10.1029/2006wr005779, n/a–n/a.
Tang, Y., Tang, Q., Tian, F., Zhang, Z., Liu, G., 2013. Responses of natural runoff to recent climatic variations in the Yellow River basin, China. Hydrol. Earth Syst. Sci. 17 (11), 4471–4480, http://dx.doi.org/10.5194/hess-17-4471-2013.
Tapley, B.D., Bettadpur, S., Watkins, M., Reigber, C., 2004. The gravity recovery and climate experiment: mission overview and early results. Geophys. Res. Lett. 31 (9), http://dx.doi.org/10.1029/2004gl019920, n/a–n/a.
Taye, M.T., Willems, P., 2013. Identifying sources of temporal variability in hydrological extremes of the upper Blue Nile basin. J. Hydrol. 499, 61–70.
Taye, M., Willems, P., Block, P., 2015. Implications of climate change on hydrological extremes in the Blue Nile basin: a review. J. Hydrol.: Reg. Stud. 4, 280–293.
Van Steenbergen, N., Willems, P., 2012. Method for testing the accuracy of rainfall-runoff models in predicting peak flow changes due to rainfall changes, in a climate changing context. J. Hydrol. 414–415, 425–434.
Wahr, J., Swenson, S., Zlotnicki, V., Velicogna1, I., 2004. Time-variable gravity from GRACE: first results. Geophys. Res. Lett. 31 (11), http://dx.doi.org/10.1029/2004gl019779.
Wang, G., Shen, Y., Cheng, G., 2000. Eco-environmental changes and causal analysis in the source regions of the Yellow River. J. Glaciol. Geocryol., 2000–03 (in Chinese with English abstract).
Wang, H., Yang, Z., Saito, Y., Liu, J.P., Sun, X., 2006. Interannual and seasonal variation of the Huanghe (Yellow River) water discharge over the past 50 years: connections to impacts from ENSO events and dams. Glob. Planet. Change 50 (3-4), 212–225, http://dx.doi.org/10.1016/j.gloplacha.2006.01.005.
Wang, Y., Wang, X., Li, C., Wu, F., Yang, Z., 2014. Spatiotemporal analysis of temperature trends under climate change in the source region of the Yellow River, China. Theor. Appl. Climatol., http://dx.doi.org/10.1007/s00704-014-1112-4.
Willems, P., 2013a. Multidecadal oscillatory behaviour of rainfall extremes in Europe. Clim. Change 120 (4), 931–944.

Willems, P., 2013b. Adjustment of extreme rainfall statistics accounting for multidecadal climate oscillations. J. Hydrol. 490, 126–133.
Wu, Q., Dong, X., Liu, Y., Jin, H., 2007. Responses of permafrost on the qinghai-tibet plateau, China, to climate change and engineering construction. Arct. Antarct. Alp. Res. 39 (4), 682–687, http://dx.doi.org/10.1657/1523-0430(07-508)[WU]2.0.CO;2.
Yang, H., Yang, D., 2011. Derivation of climate elasticity of runoff to assess the effects of climate change on annual runoff. Water Resour. Res. 47 (7), http://dx.doi.org/10.1029/2010wr009287, n/a–n/a.
Yang, D., Li, C., Hu, H., Lei, Z., Yang, S., Kusuda, T., Koike, T., Musiake, K., 2004. Analysis of water resources variability in the Yellow River of China during the last half century using historical data. Water Resour. Res. 40 (6), http://dx.doi.org/10.1029/2003wr002763, n/a–n/a.
Yang, J., Ding, Y., Liu, S., Liu, J., 2007. Variations of snow cover in the source region of the Yangtze and Yellow River in China between 1960 and 1999. J. Glaciol. 53 (182), 420–426.
Zhang, S., Jia, S., Liu, C.M., 2004a. Study on the changes of water cycle and its impacts in the source region of the Yellow River. Sci China (Ser E) 34 (Suppl. 1), 117–125, http://dx.doi.org/10.1360//04ez0012.
Zhang, Y., Li, T., Wang, B., 2004b. Decadal change of the spring snow depth over the Tibetan Plateau: the associated circulation and influence on the east summer monsoon. J. Clim. 17, 2780–2793.
Zhang, J., Li, G., Liang, S., 2012. The response of river discharge to climate fluctuations in the source region of the Yellow River. Environ.l Earth Sci. 66 (5), 1505–1512, http://dx.doi.org/10.1007/s12665-011-1390-4.
Zhang, L., Su, F., Yang, D., Hao, Z., Tong, K., 2013. Discharge regime and simulation for the upstream of major rivers over Tibetan Plateau. J. Geophys. Res. Atmos. 118, 8500–8518, http://dx.doi.org/10.1002/jgrd.50665.
Zhang, A., Zheng, C., Wang, S., Yao, Y., 2015. Analysis of streamflow variations in the Heihe River Basin northwest China: trends, abrupt changes, driving factors and ecological influences. J. Hydrol.: Reg. Stud. 3, 106–124.
Zhao, F., Xu, Z., Huang, J., 2007. Long-term trend and abrupt change for major climate variables in the upper yellow river basin. Acta Meteorol. Sin. 21 (2), 204–214.
Zhao, F., Xu, Z., Zhang, L., Zuo, D., 2009. Streamflow response to climate variability and human activities in the upper catchment of the Yellow River Basin. Sci. China Ser. E: Technol. Sci. 52 (11), 3249–3256, http://dx.doi.org/10.1007/s11431-009-0354-3.
Zheng, H., Zhang, L., Liu, C., Shao, Q., Fukushima, Y., 2007. Changes in stream flow regime in headwater catchments of the Yellow River basin since the 1950. Hydrol. Process. 21 (7), 886–893, http://dx.doi.org/10.1002/hyp.6280.
Zheng, H., Zhang, L., Zhu, R., Liu, C., Sato, Y., Fukushima, Y., 2009. Responses of streamflow to climate and land surface change in the headwaters of the Yellow River Basin. Water Resour. Res. 45, http://dx.doi.org/10.1029/2007wr006665.
Zhou, D., Huang, R., 2012. Response of water budget to recent climatic changes in the source region of the Yellow River. Chin. Sci. Bull. 57 (17), 2155–2162, http://dx.doi.org/10.1007/s11434-012-5041-2.